Inorg. Chem. **2008**, *47*, 10135−10140

Pentavalent Uranium Oxide via Reduction of $[UO_2]^{2+}$ Under Hydrothermal Reaction Conditions†

Nebebech Belai,‡ Mark Frisch,‡ Eugene S. Ilton,§ Bruce Ravel,|| and Christopher L. Cahill*,‡,⊥

Department of Chemistry, George Washington University, 725 21st Street N.W., Washington, D.C. 20052, Pacific Northwest National Laboratory, Chemical and Material Science Division, MSIN: K8-96, 902 Battelle Boulevard, Richmond, Washington 99352, National Institute of Standards and Technology, 100 Bureau Drive, Gaithersburg, Maryland 20899, and Geophysical Laboratory, Carnegie Institution of Washington, Washington, D.C. 20015

Received August 11, 2008

The synthesis, crystal structure, and spectroscopic characterization of $[U^V(H_2O)_2(U^{VI}O_2)_2O_4(OH)](H_2O)_4$ (**1**), a mixed-valent U^V/U^{VI} oxide material, are reported. The hydrothermal reaction of UO_2^{2+} with Zn and hydrazine at 120 °C for three days yields **1** in the form of a dark red crystalline solid. Compound **1** has been characterized by a combination of single-crystal and powder X-ray diffraction (XRD), elemental analysis, thermogravimetric analysis, X-ray photoelectron spectroscopy (XPS) and X-ray absorption spectroscopy (XAS). The structure consists of an extended sheet of edge and corner shared U^{VI} pentagonal bipyramids that are further connected by edge sharing to square bipyramidal U^V units. The overall topology is similar to the mineral ianthinite. The uranium L_{III}-edge XAS revealed features consistent with those observed by single-crystal X-ray diffraction. High resolution XPS data analysis of the U4f region confirmed the oxidation states of U as originally assigned from XRD analysis and bond valence summations.

Introduction

The chemistry of materials containing pentavalent uranium is significantly less developed compared to the extensive catalog of U^{IV} and U^{VI} compounds.[1−5] Synthesis of U^V materials from aqueous solution is even less evolved owing to the tendency of this species to either oxidize to U^{VI} or disproportionate to U^{IV} and U^{VI}.[4,6−9] Facile and reproducible routes to U^V containing oxide materials are particularly desirable to allow for systematic study of their structural features as well as for delineating reaction conditions where stability of this typically "overlooked" oxidation state is favorable. The latter bears significant relevance to the nuclear fuel cycle and uranium mobility/behavior in the environment.

Nature has provided us with two examples of pentavalent U-containing minerals: wyartite, $Ca[U^V(U^{VI}O_2)_2(CO_3)O_4(OH)](H_2O)_7$ and "dehydrated wyartite", $Ca(CO_3)[U^V(U^{VI}O_2)_2O_4(OH)](H_2O)_3$. These mixed-valent minerals have a layered structure with a U^{VI}/U^V ratio = 2 (Table S2, Supporting Information).[10,11] Their existence suggests that conditions to promote and stabilize the formation of U^V either exist currently, or have existed in natural settings at some point. Both of these minerals were discovered in the

† Certain commercial equipment, instruments, or materials are identified in this article in order to specify the experimental procedure adequately. Such identification is not intended to imply recommendation or endorsement by the National Institute of Standards and Technology, nor is it intended to imply that the materials or equipment are necessarily the best available for this purpose.

* To whom correspondence should be addressed. E-mail: Cahill@gwu.edu.
‡ George Washington University.
§ Pacific Northwest National Laboratory.
|| National Institute of Standards and Technology.
⊥ Carnegie Institution of Washington.

(1) Szabé, Z.; Toraishi, T.; Vallet, V.; Grenthe, I. *Coord. Chem. Rev.* **2006**, *250*, 784–815.
(2) Burns, C. J.; Neu, M. P.; Boukhalfa, H.; Gutowski, K. E.; Bridges, N. J.; Rogers, R. D. In *The Actinides. Comprehensive Coordination Chemistry II*; McCleverty, J. A., Meyer, T. J., Eds.; Elsevier: Oxford, 2004; Vol. *3*, pp 189−345.
(3) Katz, J. J.; Seaborg, G. T.; Morss, L. R., Eds. *The Chemistry of the Actinide Elements*, 2nd ed.; Chapman and Hall: London, 1986.
(4) Selbin, J.; Ortego, J. D. *Chem. Rev.* **1969**, *69*, 657–671.
(5) Clark, D. L.; Hobart, D. E.; Neu, M. P. *Chem. Rev.* **1995**, *95*, 25–48.
(6) Kraus, K. A.; Nelson, F. *J. Am. Chem. Soc.* **1949**, *71*, 2517–2522.
(7) Kraus, K. A.; Nelson, F.; Johnson, G. L. *J. Am. Chem. Soc.* **1949**, *71*, 2510–2517.
(8) Ekstrom, A. *Inorg. Chem.* **1974**, *13*, 2237–2241.
(9) Nelson, F.; Kraus, K. A. *J. Am. Chem. Soc.* **1951**, *73*, 2157–2161.
(10) Hawthorne, F. C.; Finch, R. J.; Ewing, R. C. *Can. Mineral.* **2006**, *44*, 1379–1385.
(11) Burns, P. C.; Finch, R. J. *Am. Mineral.* **1999**, *84*, 1456–1460.

10.1021/ic801534m CCC: $40.75
Published on Web 10/09/2008

Shinkolobwe mine in the Democratic Republic of Congo as alteration products of uraninite ($U^{IV}O_2$). As such, we surmised that mild hydrothermal treatment with appropriate control or influence of oxidizing/reducing conditions would be a viable route to analogous synthetic materials.

A review of synthetic efforts to produce U^V compounds shows that in recent years, several U^V containing complexes and materials have been synthesized through oxidation of U^{IV} or other low-valent uranium compounds.[12−19] In addition, several U^V compounds were isolated via reduction of the uranyl (UO_2^{2+}) cation or U^{VI} starting compounds.[20−22] Most of these oxidation or reduction reactions were carried out in organic solvents under oxygen-free conditions. Furthermore, oxidation of U^{IV} and U^{III} precursors under nonaqueous or controlled hydrolysis conditions has led to the isolation of large polyoxo uranium clusters containing U^V, suggesting that these alternate synthetic conditions prevent the formation of trans-dioxouranyl (UO_2^{2+}) compounds hence resulting in new types of coordination and stabilization of U^V.[23,24] A U^V silicate reported in Lii et al. was synthesized using a hydrothermal synthesis; however, the reaction was carried out at a much higher temperature (600 °C) than the conditions reported in this contribution.[25] Additionally, a number of U^V complexes have been prepared in aqueous solution through electrochemical or photochemical reduction of hexavalent precursors and stabilized by coordination with carbonate or organic ligands.[26−34] Mixed valent and monovalent U^V containing alkali uranates have been synthesized using solid-state methods and controlled gas mixtures at elevated temperatures, as recently exemplified by the XAS study of Soldatov et al.[35] Pentavalent species have also been formed by in situ reduction of UO_2^{2+} cations on the surface of ferrous mica.[36] Spectroscopic studies of the latter in particular require detailed crystallographic information (as provided herein) to correlate observations to structural features.

Much of the focus and impetus for the study of U^V materials and indeed U-redox in general has centered around the nuclear fuel cycle and environmental concerns. In particular, relevance to long-term storage of spent nuclear fuel has driven efforts to synthesize U^V compounds to study their stability, physiochemical properties, and role(s) as intermediate species in uranium redox reactions.[37−39] Uranium is the primary component (by mass) of spent nuclear fuel from commercial reactors and its release into the environment during long-term storage is a major concern, especially when considering that U^{VI} is highly soluble in water. In this study, we show that under narrow range of conditions including pH, temperature and judicious choice of reducing agent, it is possible to isolate pentavalent uranium from aqueous (1:1 water/acetonitrile) solution and produce a stable uranium-(hydr)oxide compound under mild hydrothermal conditions without the incorporation of carbonate, silicate, or organic ligands. The synthesis and characterization of $[U^V(H_2O)_2(U^{VI}O_2)_2O_4(OH)](H_2O)_4$ (**1**), by single-crystal and powder X-ray diffraction, X-ray photoelectron spectroscopy (XPS), X-ray absorption spectroscopy (XAS), thermogravimetric analysis (TGA), elemental analysis, and infrared spectroscopy (IR), are presented herein.

Experimental Section

Synthesis of $[U^V(H_2O)_2(U^{VI}O_2)_2O_4(OH)](H_2O)_4$. Uranium acetate ($UO_2(CH_3COO)_2 \cdot 2H_2O$) and zinc metal (powder) were obtained from Fisher Scientific, and hydrazine dihydrochloride ($N_2H_4 \cdot 2HCl$) was acquired from Sigma Aldrich. *Although the uranium oxyacetate used contains depleted uranium, standard safety measures for handling radioactive substance should be followed.* Compound **1** was synthesized by heating a mixture of $UO_2(CH_3COO)_2 \cdot 2H_2O$ (0.30 g), Zn (0.015 g), and $N_2H_4 \cdot 2HCl$ (0.25 g,) in a 3:1:1 molar ratio in a 1:1 solution of water/acetonitrile (6 mL, pH adjusted to 1.14 using concentrated HCl) at 120 °C for three days. The reaction vessel was allowed to cool slowly to room

(12) Chondroudis, K.; Kanatzidis, M. G. *J. Am. Chem. Soc.* **1997**, *119*, 2574–2575.
(13) Salmon, L.; Thuéry, P.; Ephritikhine, M. *Polyhedron* **2007**, *26*, 631–636.
(14) Gray, D. L.; Backus, L. A.; Krug von Nidda, H.-A.; Skanthakumar, S.; Loidl, A.; Soderholm, L.; Ibers, J. A. *Inorg. Chem.* **2007**, *46*, 6992–6996.
(15) Graves, C. R.; Scott, B. L.; Morris, D. E.; Kiplinger, J. L. *J. Am. Chem. Soc.* **2007**, *129*, 11914–11915.
(16) Arliguie, T.; Fourmigué, M.; Ephritikhine, M. *Organometallics* **2000**, *19*, 109–111.
(17) Burdet, F.; Pécaut, J.; Mazzanti, M. *J. Am. Chem. Soc.* **2006**, *128*, 16512–16513.
(18) Natrajan, L.; Burdet, F.; Pécaut, J.; Mazzanti, M. *J. Am. Chem. Soc.* **2006**, *128*, 7152–7153.
(19) Arnaudet, L.; Bougon, R.; Buu, B.; Lance, M.; Nierlich, M.; Vigner, J. *Inorg. Chem.* **1994**, *33*, 4510–4516.
(20) Berthet, J.-C.; Siffredi, G.; Thuéry, P.; Ephritikhine, M. *Chem. Comm.* **2006**, 3184–3186.
(21) Berthet, J.-C.; Nierlich, M.; Ephritikhine, M. *Angew. Chem., Int. Ed.* **2003**, *42*, 1952–1954.
(22) Duval, P. B.; Burns, C. J.; Buschmann, W. E.; Clark, D. L.; Morris, D. E.; Scott, B. L. *Inorg. Chem.* **2001**, *40*, 5491–5496.
(23) Duval, P. B.; Burns, C. J.; Clark, D. L.; Morris, D. E.; Scott, B. L.; Thompson, J. D.; Werkema, E. L.; Jia, L.; Andersen, R. A. *Angew. Chem., Int. Ed.* **2001**, *40*, 3357–3361.
(24) Nocton, G.; Burdet, F.; Pécaut, J.; Mazzanti, M. *Angew. Chem., Int. Ed.* **2007**, *46*, 7574–7578.
(25) Chen, C.-S.; Lee, S.-F.; Lii, K.-H. *J. Am. Chem. Soc.* **2005**, *127*, 12208–12209.
(26) Ikeda, A.; Hennig, C.; Tsushima, S.; Takao, K.; Ikeda, Y.; Scheinost, A. C.; Bernhard, G. *Inorg. Chem.* **2007**, *46*, 4212–4219.
(27) Morris, D. E.; Da Re, R. E.; Jantunen, K. C.; Castro-Rodriguez, I.; Kiplinger, J. L. *Organometallics* **2004**, *23*, 5142–5153.
(28) Mizuoka, K.; Grenthe, I.; Ikeda, Y. *Inorg. Chem.* **2005**, *44*, 4472–4474.
(29) Mizuoka, K.; Ikeda, Y. *Inorg. Chem.* **2003**, *42*, 3396–3398.
(30) Mizuoka, K.; Kim, S.-Y.; Hasegawa, M.; Hoshi, T.; Uchiyama, G.; Ikeda, Y. *Inorg. Chem.* **2003**, *42*, 1031–1038.
(31) Mizuoka, K.; Tsushima, S.; Hasegawa, M.; Hoshi, T.; Ikeda, Y. *Inorg. Chem.* **2005**, *44*, 6211–6218.
(32) Docrat, T. I.; Mosselmans, J. F. W.; Charnock, J. M.; Whiteley, M. W.; Collison, D.; Livens, F. R.; Jones, C.; Edmiston, M. J. *Inorg. Chem.* **1999**, *38*, 1879–1882.
(33) Roussel, P.; Hitchcock, P. B.; Tinker, N. D.; Scott, P. *Inorg. Chem.* **1997**, *36*, 5716–5721.
(34) Howes, K. R.; Bakac, A.; Espenson, J. H. *Inorg. Chem.* **1988**, *27*, 791–794.
(35) Soldatov, A. V.; Lamoen, D.; Konstantinović, M. J.; Van den Berghe, S.; Scheinost, A. C.; Verwerft, M. *J. Solid State Chem.* **2007**, *180*, 53–60.
(36) Ilton, E. S.; Haiduc, A.; Cahill, C. L.; Felmy, A. R. *Inorg. Chem.* **2005**, *44*, 2986–2988.
(37) Grobmann, K.; Arnold, T.; Krawczyk-Bärsch, E.; Diessner, S.; Wobus, A.; Bernhard, G.; Krawietz, R. *Environ. Sci. Technol.* **2007**, *41*, 6498–6504.
(38) Morss, L. R.; Edelstein, N. M.; Fuger, J., Eds. *The Chemistry of the Actinide and Transactinide Elements*, 3nd ed.; Springer: Dordrecht, 2006.
(39) Ewing, R. C. *Can. Mineral.* **2001**, *39*, 697–715.

temperature. Dark red needle crystals were obtained after decanting the dark reaction solution (pH = 3.50). The crystals were sonicated and washed first with water followed by a water/ethanol solution, ethanol, and finally with acetone. The crystals were then allowed to dry completely at room temperature. Yield: 51% based on uranium. Elemental analysis (was performed by Galbraith Laboratories at Knoxville, Tennessee), observed (calculated): U 70.6% (73.8%); Zn 227 ppm; C 1.53%; H 1.00%; N 0.80%. IR (KBr, cm^{-1}): ν(U−O) 915 (s), 803 (w), 790 (w), 659 (w), 574 (m), 456 (m).

Crystallographic Studies. A dark red needle of $[U^{V}(H_2O)_2(U^{VI}O_2)_2O_4(OH)](H_2O)_4$ was mounted on a glass fiber and a hemisphere of data (12086 reflections) were collected at room temperature with a Bruker SMART diffractometer equipped with an APEX II CCD detector using Mo Kα radiation (λ = 0.7103 Å) and both φ and ω scans. The determination of intensities and cell refinement were performed with the Bruker SAINT software package and a semiempirical absorption correction was applied using SADABS.[40,41] The structure was solved in an orthorhombic space group *Immm* using direct methods and was refined using SHELX-97 within the WinGX software suite.[42,43] The heavy atoms and all non-hydrogen atoms in the structure were found using Fourier difference maps and ultimately refined anisotropically.

X-ray Powder Diffraction (XRD). Powder X-ray diffraction data was collected on a Rigaku Miniflex II (Cu Kα, 3−60° in 2θ, 0.05° step, 1.0 s/step) and data was manipulated using JADE.[44] Samples for XRD were prepared by first grinding the sample with acetone and then spreading a slurry mixture on a zero-background sample support to create a thin layer of powder.

Thermogravimetric Analysis (TGA). Thermogravimetric analysis was collected on a Perkin-Elmer Pyris1. Sample **1** was heated from 30 to 900 °C at 10 deg min^{-1} under a N_2 gas flow. The TGA on **1** shows a weight loss of approximately 10% between 50−500 °C (Supporting Information). These correspond to loss of the interlayer water (calculated, 7.4%) and to loss of bound water ligands on U1 (calculated, 3.8%) for a total theoretical weight loss of 11.2%. The mixture of products formed at 900 °C, U_3O_8 (31−1424) and UO_3 (31−1417), representing a final weight percent of 87.1% for U_3O_8 and 88.7% for UO_3, and are in good agreement with loss of all 6 water molecules for **1** in the experimental data.

X-ray Photoelectron Spectroscopy (XPS). A Scienta ESCA300 that employs a high flux monochromatic Al Kα X-ray beam was used to obtain the XPS data which was then used to establish the two oxidation states of uranium in **1** as described previously.[36,45] Operational conditions yielded a Fermi edge width = 0.41 eV for Ag. The binding energy scale was referenced to adventitious C1s at 285.0 eV. U4f spectra were best fit by nonlinear least-squares. For the most reduced samples, as measured by XPS, a Shirley background was used and extended from about 8 eV below the $4f_{7/2}$ peak to about 15 eV above the $4f_{5/2}$ peak. This binding energy (BE) spread encompassed the primary peaks and major satellite features. The BEs and heights for individual components (satellites and primary peaks) were allowed to move as a packet relative to the other components (i.e., satellite-primary peak BE separations and relative heights were fixed for a given component). Schoepite and UO_2 (formed by reduction of U^{VI}aq with green rust, a $Fe^{II}-Fe^{III}$ oxyhydroxide) were used as the U^{VI} and U^{IV} standards, respectively. A single, but variable full-width at half-maximum (fwhm) was used for all the primary peak components. Satellite and core peak FWHMs were set at a fixed ratio for each component. In order to avoid local minima, optimum fits were approached by varying the initial abundance of the components. A combination of U^{VI} and U^{IV} did not fit the spectra well. Fitting with the U^{VI} standard and solving for the second component yielded a component spectrum with primary peaks at ~1 eV lower binding energy than for U^{VI} and associated satellites at 8.3 eV above the main component peaks. These features are diagnostic of U^{V}.[46] The energy resolution obtained by the Scienta300, combined with tightly correlating primary peaks to their corresponding satellites, imposed severe constraints on curve fitting. For samples that showed substantial surface oxidation, the Shirley background tended to over subtract intensity between the spin orbit split peaks. In such cases, the background was tightly wrapped around the $4f_{7/2}$ peak, and the satellite structure was only used to qualitatively identify the oxidation states of U. Because the satellite/primary peak intensity ratio is greater for U^{V} than U^{VI}, U^{V} was likely underestimated by 5−10% for more oxidized samples.

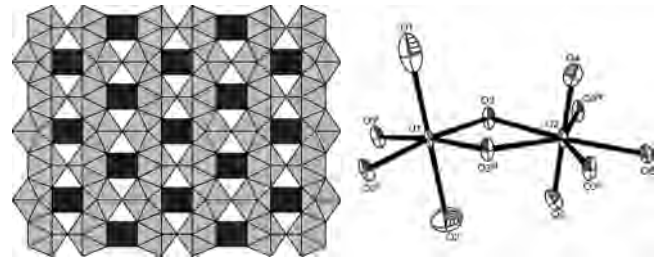

Figure 1. Extended sheet structure of $[U^{V}(H_2O)_2(U^{VI}O_2)_2O_4(OH)](H_2O)_4$ viewed down [001] and local coordination for the U^{V} and U^{VI} sites. In the sheet U1 sites are in dark gray square bipyramidal polyhedra and U2 sites are in gray pentagonal bipyramidal polyhedra. Symmetry codes: $i = x, -y, z$; ii = $-x, -y, z$; iii = $-x, y, z$; iv = $-x + 1/2, -y + 1/2, -z + 1/2$; $v = x + 1/2, -y + 1/2, -z + 1/2$.

X-ray Absorption Spectroscopy (XAS). Crystalline samples of **1** were ground to a fine powder with grains much smaller than the approximate absorption length of 30 μm above the U L_{III} edge.[47] The fine powder was dispersed in boron nitride and packed into a polycarbonate frame. XAS data were measured in the transmission geometry at beamline X23A2 at the National Synchrotron Light Source using a Si(311) monochromator. Argon-filled ionization chambers were used to measure the incident and transmitted intensities and the U^{VI} sample shown in Figure 3 was measured in parallel as a calibration and alignment standard. The data were processed using the ATHENA program.[48,49] Ten scans were aligned and averaged to yield the data shown here. The background function was found using the AUTOBK algorithm.[50]

The isolated χ(k) spectrum were then analyzed using theoretical standards from FEFF6.[51] FEFF6 was run for each uranium site in the refined structure and the scattering paths contributing from each

(40) *Area-Detector Absorption Correction*; Siemens Industrial Automation, Inc.: Madison, WI, 1996.
(41) *SAINT, Area-Detector Integration Software*; Siemens Industrial Automation, Inc.: Madison, WI, 1998.
(42) Farrugia, L. J. *J. Appl. Crystallogr.* **1999**, *32*, 837–838.
(43) Sheldrick, G. M. *Programs for Crystal Structure Analysis (Release 97-2)*; University of Göttingen: Germany .
(44) *Jade 6.1 ed.*; Materials Data Inc.: Livermore, CA 2002.
(45) Ilton, E. S.; Haiduc, A.; Moses, C. O.; Heald, S. M.; Elbert, D. C.; Veblen, D. R. *Geochim. Cosmochim. Acta* **2004**, *68*, 2417–2435.
(46) Ilton, E. S.; Boily, J.-F.; Bagus, P. S. *Surf. Sci.* **2007**, *601*, 908–916.
(47) Stern, E. A.; Kim, K. *Phys. Rev.* **1981**, *B23*, 3781–3787.
(48) Ravel, B.; Newville, M. *J. Synchrotron Rad.* **2005**, *12*, 537–541.
(49) Newville, M. *J. Synchrotron Rad.* **2001**, *8*, 322–324.
(50) Newville, M.; Livins, P.; Yacoby, Y.; Rehr, J. J.; Stern, E. A. *Phys. Rev.* **1993**, *B47*, 14126–14131.
(51) Zabinsky, S. I.; Rehr, J. J.; Ankudinov, A.; Albers, R. C.; Eller, M. J. *Phys. Rev.* **1995**, *B52*, 2995–3009.

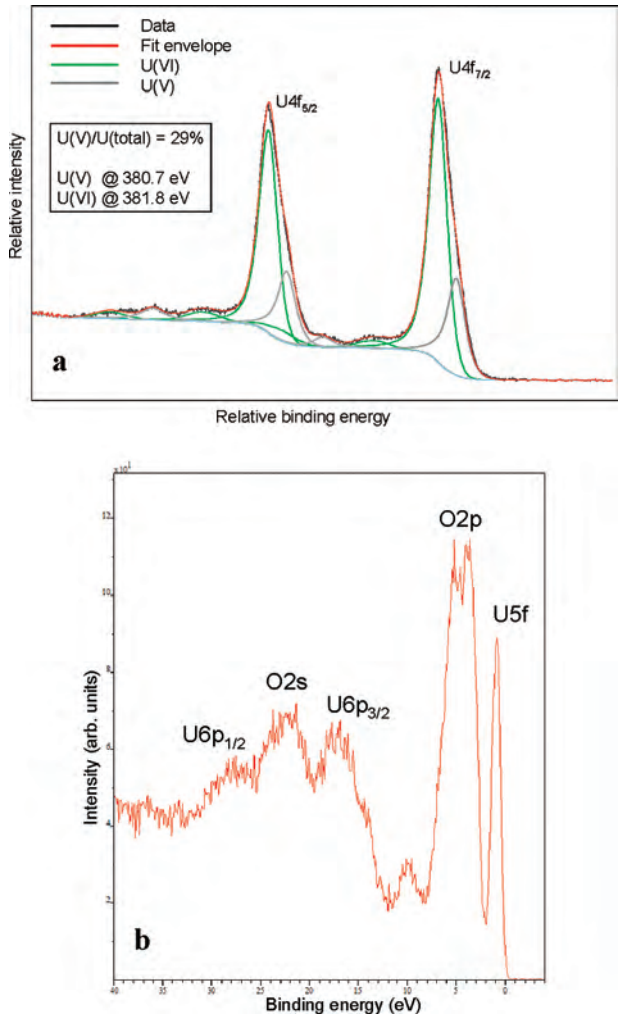

Figure 2. XPS spectra of $[U^{V}(H_2O)_2(U^{VI}O_2)_2O_4(OH)](H_2O)_4$. (a) Uranium 4f region and the result of U 4f fitting. (b) Valence band region.

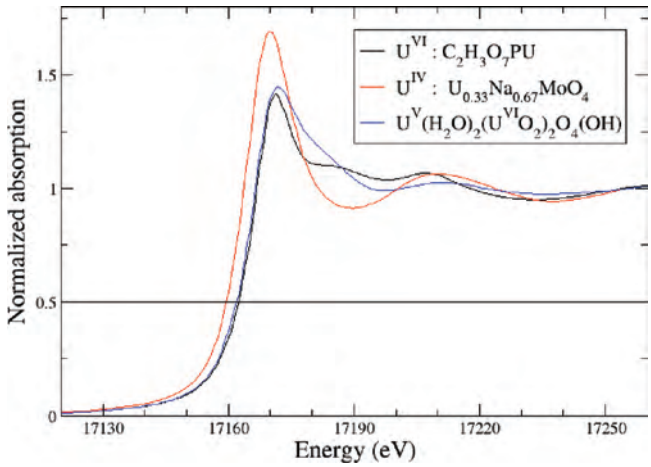

Figure 3. Calibrated, aligned, and normalized XANES data for U^{VI} (black) and U^{IV} (red) species along with the mixed valence $U^{VI/V}$ species (blue).

site were weighted by stoichiometry in the analysis. This is a fairly disordered structure, with most coordination shells split into two or more subshells. Even with the high quality data obtained in this measurement, the information content of the extended X-ray absorption fine structure (EXAFS) signal is not adequate to refine distance and mean square displacement parameters for each scatterer individually. With a Fourier transform range of 3−12 $Å^{-1}$ and a fitting range from 1.0−4.2 Å, we have an upper limit of 18 independent points in these data. Constraints among the fitting parameters are required and the parameters used in the fit are listed in Supporting Information, Table S1.

The assignment of Δr and σ^2 parameters to groups of similar scatterers at different distances and in different locations in the crystal structure is only an approximation and is a major source of systematic error in the analysis. However, these simple constraints allowed a reasonable analysis to proceed, using only 11 variable parameters. When floated, the S_0^2 parameter was consistent with 1, so it was fixed at one in this analysis, following the lead in Kelly et al.[52] With the one exception discussed above, all parameters are physically reasonable.

Results and Discussion

Synthesis. Compound **1** was synthesized by heating a mixture of uranium oxyacetate, zinc powder, and hydrazine dihydrochloride in a 3:1:1 molar ratio into a 1:1 solution of water/acetonitrile at 120 °C for three days. This synthesis is reproducible, having been repeated over a dozen times successfully in our laboratory. The product is relatively stable for months under ambient conditions, although surface oxidation over time has been detected by XPS. This slow oxidation was not detected by powder X-ray diffraction analysis; that is, no major difference was observed between powder patterns of old and fresh samples. The partial reduction of uranium to give $2U^{VI}$ and $1U^{V}$ was only achieved in 1:1 water/acetonitrile mixed solvent and attempts to reproduce the same reaction in just water, acetonitrile, or other mixed solvents such as water/tetrahydrofuran and water/dimethylformamide have been unsuccessful thus far. Stabilization of pentavalent uranium has also been seen in other systems using acetonitrile.[21,24] In addition, given the high uranyl concentration in solution, it is possible that the synthesis of **1** was aided by the formation of aqueous $U^{VI}-U^{V}$ dimers which are known to decrease the rate of UO_2^+ disproportionation.[53]

Structural Characterization. The structure of **1** (Figure 1) consists of an extended uranium oxide sheet constructed from two symmetrically distinct U sites, U1 square bipyramidal (UO_6, dark gray polyhedra) and U2 pentagonal bipyramidal (UO_7, gray polyhedra), which are linked to one another by edge and corner sharing. The UO_7 center consists of two shorter (1.784, 1.788 Å) axial U═O bonds, forming a nearly linear UO_2^{2+} group (179.0°), and five longer (2.312−2.393 Å) equatorial U−O bonds, a typical coordination environment seen for the uranyl ion. In contrast, the UO_6 site is made of four shorter equatorial (2.059 Å) and two longer axial (2.410, 2.438 Å) U−O bonds resulting in a local geometry significantly different from the UO_2^{2+} cation. Details of the data collection and refinement can be found in Table 1, and additional details are available as a CIF data in Supporting Information

(52) Kelly, S. D.; Kemner, K. M.; Fein, J. B.; Fowle, D. A.; Boyanov, M. I.; Bunker, B. A.; Yee, N. *Geochim. Cosmochim. Acta* **2002**, *66*, 3855–3871.
(53) Arland, S. In *The Chemistry of the Actinide Elements*, 2nd ed.; Katz, J. J., Seaborg, G. T., Morss, L. R., Eds.; Chapman and Hall: London, 1986; Vol. *2*, pp 1480−1546.

Table 1. Crystallographic Data for $[U^V(H_2O)_2(U^{VI}O_2)_2O_4(OH)](H_2O)_4$

formula	$U_3O_{14}H_5$ (interlayer water molecules not included)
formula mass (amu)	894.11
space group	*Immm* (No. 71)
a (Å)	7.1757 (9)
b (Å)	11.4000 (15)
c (Å)	15.310 (2)
$\alpha = \beta = \gamma$ (deg)	90.00
V (Å^3)	1252.4 (3)
Z	4
T (K)	293 (2)
θ range (deg)	2.23−30.37
λ (Å)	0.71073
ρ_{calcd} (Mg/m^3)	4.721
μ (mm^{-1})	38.728
goodness-of-fit, all data	1.080
largest difference peak and hole (e Å^3)	3.870 and −1.749
R_1[a]	0.0374
wR_2[b]	0.0764

[a] $R_1 = \{\sum||F_0| - |F_c||\}/\{\sum|F_0|\}$. [b] $wR_2 = \{\sum[w(F_0^2 - F_c^2)^2]/\sum[w(F_0^2)^2]\}^{1/2}$.

.

Bond valence summations were used to correlate the single crystal structure data and uranium oxidation states. Using the parameters from Burns et al., $R_{ij} = 2.051$ Å and $b = 0.519$ Å, the sum of bond valences incident at U2 and U1 sites were 6.07 and 4.91 v.u., respectively (Table S2, Supporting Information).[54] These values correspond to hexavalent and pentavalent uranium cations. The oxide sheet charge balance is preserved by bridging equatorial hydroxyl ions O6 at the U2 local configuration (shared by two corner sharing U^{VI} centers, Figure S5, Supporting Information). The two axial oxygen atoms of U1, O1 and O2 are water molecules and form a linear (180°) UO_2^+ ion. The bond valence sum (BVS) values for O1, O2, and O6 were calculated to be 0.47, 0.50, and 1.21 v.u., respectively. Since additional electron density was observed in the interlayer region, the SQUEEZE routine within the program PLATON was used to calculate the volume of any available void space in the structure.[55,56] SQUEEZE found ∼160 Å^3 of solvent accessible void per formula unit, corresponding to approximately four water molecules (40 Å^3/H_2O), however these were not located due to disorder. Further, a few residual molecules of acetonitrile may be present as well as indicated by the elemental analysis (above). Thermogravimetric analysis of **1** revealed a roughly 10% weight loss between 50−500 °C. This weight loss event corresponds to up to six water molecules (Figure S2, Supporting Information). Upon heating to 900 °C, **1** yielded a mixture of U_3O_8 and UO_3.

The sheet topology as well as the location and local geometry of the reduced uranium site in **1** are similar to ianthinite ($[(U_2^{IV}(UO_2)_4O_6(OH)_4(H_2O)_4](H_2O)_5$) which consists of U^{IV} and U^{VI}.[57] The equatorial bond lengths of the octahedral U^{IV} site in ianthinite range from 2.346−2.538 Å; the axial U−O bond lengths vary by a wider range from 1.964−2.355 Å (Table S2, Supporting Information). This is in contrast however to the structure of wyartite or dehydrated wyartite.[10,11] The U^V site in both types of wyartite is pentagonal bipyramid and the CO_3^{2-} ion is incorporated as a ligand (the CO_3^{2-} in dehydrated wyartite is disordered with a hydroxide ion). The U−O axial and equatorial bond lengths measured for U1 are comparable to the U^V bonds found in dehydrated wyartite. The U−O bond distances in dehydrated wyartite range from 2.09 to 2.50 Å. The axial bonds in wyartite average to 2.08 Å while the equatorial bond lengths range from 2.06−2.48 Å. The axial and equatorial bond lengths of U1 in **1**, however, are notably different than those reported for $K(UO)Si_2O_6$ and $[UO_2(OPPh_3)_4](OTf)$, both U^V compounds with comparable U^V local geometry.[21,25] The $K(UO)Si_2O_6$, a pentavalent-uranium silicate, contains a U^VO_6 octahedron with U−O equatorial bond lengths at 2.164 Å and axial bond lengths at 2.065 Å (average). In the molecular complex $[UO_2(OPPh_3)_4](OTf)$, the U^VO_6 contains U−O equatorial and axial bond lengths (both average) at 2.438 Å and 1.819 Å, respectively. Similarly, the U1 metal center in **1** has longer axial and shorter equatorial U−O bond lengths than those determined by EXAFS for the U^V carbonate anion, $[UO_2(CO_3)_3]^{5-}$.[32] Lastly, we highlight an unusually short interlayer distance of 1.98 Å between water molecules bound to U1 sites on opposite sheets.

XPS Analysis. High resolution XPS was used to further establish the oxidation states of uranium in **1**. Curve fitting of the U4f region indicated the presence of two components consistent with U^V and U^{VI} (Figure 2a), in support of the BVS values obtained from the single-crystal diffraction analysis. This conclusion is supported by the binding energies of the components as well as the satellite structure (see Experimental Section). Importantly, there was no evidence for U^{IV}. Further, the presence of a strong U5f peak in the valence band region (Figure 2b) records the presence of reduced U, which excludes the possibility that the low binding energy component is a U^{VI}-uranate species, which can have binding energies that overlap with U^V. For some samples, sequential analyses indicated slow systematic reduction of U^{VI} under the beam. In such cases, U^V/U(total) values were obtained by extrapolating to time zero. The XPS determined U^V/U(total) ratio in different samples ranged from 17 to 29%. This contrasts with the single crystal data which consistently indicated U^V/U(total) = 33%. Grinding of the same sample tended to increase the measured XPS U^V/U(total) ratio, suggesting the near surface of the compound was more oxidized than the bulk.

EXAFS Analysis. X-ray absorption spectroscopy is a direct measure of the oxidation state and local structure around ions. The uranium L_{III}-edge X-ray absorption spectra of compound **1**were analyzed and the results are consistent with the XPS and X-ray diffraction results. The X-ray absorption near edge structure (XANES) data for **1** and for U^{IV} and U^{VI} reference materials is shown in Figure 3. The two reference materials are $U_{0.33}Na_{0.67}MoO_4$, a scheelite type material, and $(UO_2)(O_3PCH_2CO_2H)$, a uranium phosphate material; both were synthesized in our laboratory and contain

(54) Burns, P. C.; Ewing, R. C.; Hawthorne, F. C. *Can. Mineral.* **1997**, *35*, 1551–1570.
(55) van der Sluis, P.; Spek, A. L. *Acta Crystallogr.* **1990**, *A46*, 194–201.
(56) Spek, A. L. *Acta Crystallogr.* **1990**, *A46* (Supplement), C34.
(57) Burns, P. C.; Finch, R. J.; Hawthorne, F. C.; Miller, M. L.; Ewing, R. C. *J. Nucl. Mater.* **1997**, *249*, 199–206.
(58) $(UO_2)(O_3PCH_2CO_2H)$. Synthesis and crystal structure details are in Cahill et al. *Inorg. Chem.* **2008,** *47*, 7660–7672.

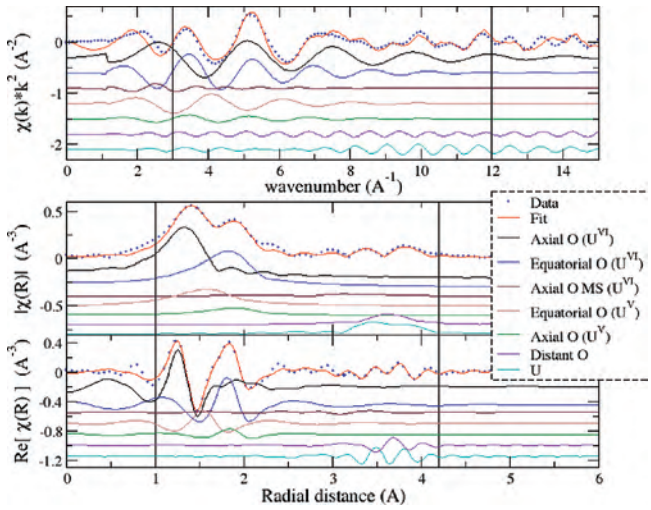

Figure 4. The k^2-weighted $\chi(k)$ data (top) and the magnitude (middle) and real part (bottom) of its Fourier transform along with the fit and the contributions from the various types of scatterers. The vertical lines indicate the Fourier transform range in k and the fitting range in R.

only U^{IV} and U^{VI}, respectively.[58,59] The XANES data for U^{VI} and U^{IV} species show the characteristic features of those valences, including the pronounced shoulder 17185 eV for U^{VI} and a strong white line for U^{IV}. The U^{VI} edge, measured as the position of the half-edge step marked by the horizontal line, is at 17162.4 eV, a characteristic 2.9 eV above[60] the U^{IV} edge at 17159.5 eV. The edge of the mixed valence species is at 17162.0 eV, a value which is consistent with a mixed U^V/U^{VI} material. Soldatov et al. also noted that the L_{III}-edges for U^V alkali oxides were intermediate to the L_{III}-edges for U^{VI} and U^{IV} alkali oxides.[35]

The fit to the extended X-ray absorption fine structure (EXAFS) is shown in Figure 4 with results given in Table S1, Supporting Information. There are several interesting aspects of this fit. First, the equatorial U^V-O bond at 2.094(039), which is slightly longer than, but within error of, the value obtained from single-crystal X-ray diffraction analysis, is essential to fitting the peaks between 1 and 2.2 Å. Although this split peak resembles what is seen for U^{VI} species,[52] a fit to these data is very poor if that intermediate length U−O bond is excluded. Second, the bulk of the misfit is contained in the region between 2.2 and 3.2 Å. Related to that is the unphysical value of σ^2 obtained for the group of distant O scatterers. This misfit and the unphysical parameter value suggest the presence of local structure or disorder which is visible in the EXAFS but which is of sufficiently short correlation length that it cannot be seen in the X-ray structure refinement of the crystallography data. This could be due to rotations of the U−O structural units in the vicinity of oxygen vacancies or by the presence of water retained between the structural sheets. Using the U−O distances obtained from the fit, bond valence sums were calculated, yielding 4.64(15) for the U^V site and 6.65(5) for the U^{VI} site, which differ only by about 1/2 valence unit from the results of the X-ray structure refinement. This systematic inaccuracy can be attributed to the constraints placed on the fitting parameters.

The XANES results shown in Figure 4 and the bond valence summations computed from the EXAFS fit results are consistent with the presence of ordered U^V in this material. The EXAFS analysis demonstrates that the structure obtained from the X-ray structure refinement is largely consistent with the measured local structure, although there is evidence of local distortion due possibly to oxygen vacancies or to the presence of interlayer water.

Conclusion

We have reported a stable U^V/U^{VI} compound synthesized through partial reduction of the UO_2^{2+} cation in aqueous solution. The structure and the uranium oxidation states of **1** were confirmed by single-crystal X-ray diffraction, X-ray photoelectron spectroscopy and X-ray absorption spectroscopy. The stabilization of U^V was promoted in the water/acetonitrile solvent system most likely by the formation of $U^{VI}-U^V$ dimers, hence decreasing the rate/extent of UO_2^+ disproportionation. If this suggestion is valid, exploring related reactions under similarly reducing and mild hydrothermal conditions (as opposed to starting from U^{IV}) should provide a general route to the formation and stabilization of hydrated pentavalent U materials without the need for the incorporation of carbonate, silicate, or organic ligands.

Acknowledgment. This work was supported by funding from the U.S. Department of Energy (DOE), under grant DE-FG02-05ER15736 at GWU and from The National Science Foundation (DMR-0419754 and DMR-0348982). Use of the National Synchrotron Light Source, Brookhaven National Laboratory, was supported by the DOE, Office of Science, Office of Basic Energy Sciences, under Contract No. DE-AC02-98CH10886. Research at Pacific Northwest National Laboratory was supported by the Geosciences Research Program, Office of Basic Energy Sciences, and DOE. We further acknowledge the allocation of time and services in the SCIENTA ESCA laboratory of Lehigh University. Professional and technical guidance of Dr. Alfred C. Miller is greatly appreciated.

Supporting Information Available: X-ray crystallographic file for compound **1** in CIF format, X-ray powder diffraction patterns, TGA report, fitting parameters used for EXAFS, and IR spectrum are available free of charge via the Internet at http://pubs.acs.org.

IC801534M

(59) $U_{0.33}Na_{0.67}MoO_4$. Uranium oxyacetate (0.0717g, 0.169 mmol) was added to a freshly prepared 0.1 M solution of $\{Mo^V_2O_4\}^{2+}$ (3.0 mL) [dimers prepared as in Dolbecq et al. *Inorg. Chem.* **2006** *45*, 5898−5910] and the pH of the solution was adjusted to 6.36 using a 4 M NaOH solution. The dark orange turbid solution was sealed in a 23 mL Teflon-lined Parr bomb and heated for four days at 150 °C. The reaction mixture was then allowed to cool to room temperature. The black cloudy solution (final pH = 5.44) was decanted and the resulting dark orange crystals of $U_{0.33}Na_{0.67}MoO_4$ were washed repeatedly with water followed by a 1:1 water and ethanol solution. Yield: 50 mg. Publication of this material is in preparation.

(60) O'Laughlin, E. J.; Kelly, S. D.; Cook, R. E.; Csencsits, R.; Kemner, K. *Environ. Sci. Technol.* **2003**, *37*, 721–727.